Optics Communications 466 (2020) 125600

Contents lists available at ScienceDirect

Optics Communications

journal homepage: www.elsevier.com/locate/optcom

Performance analysis of RoFSO links with spatial diversity over combined channel model for 5G in smart city applications

Abhishek Kumar *, Prabu Krishnan *

Department of Electronics and Communication, National Institute of Technology Karnataka, Surathkal, Mangalore 575025, India

ARTICLE INFO

Keywords:
5G
IOT
RoFSO
Smart city
WOC

ABSTRACT

The smart city concept improves the lives of citizens and optimizes the efficiency of city operations, services through the integration of information and communication technology with the help of the internet of things (IoT) and 5G techniques. The bandwidth demand for 5G, smart city, and IoT applications are fulfilled with wireless optical communications. Particularly, radio over free space optical (RoFSO) communication establishes a very attractive choice for interconnecting central base stations with remote antenna units. In this paper, we consider the transmission of orthogonal frequency division multiplexing (OFDM) radio signals with quadrature amplitude (QAM) modulation format through a free space optical link using spatial diversity mitigation technique. The atmosphere is modeled as the combined channel model which takes into account atmospheric attenuation, turbulence, and pointing errors. The atmospheric turbulence and pointing errors are modeled by Malaga, Beckmann, and Rayleigh distributions. The novel closed form BER expressions are derived for the proposed QAM OFDM RoFSO link with spatial diversity. The results are analyzed and plotted for different weather conditions (clear, haze, light fog), turbulence regimes (weak, moderate, strong), misalignment (weak, enhanced), the order of QAM and number of transceivers. The proposed RoFSO system is highly useful for 5G in smart city applications.

1. Introduction

The whole smart city concept is based on the integration of information and communication technology. Smart city concept is imagined for the best utilization of the available resources. Internet of things (IoT) is basically connecting any device to the internet and controlling its functions through commands from the internet. So, for making the smart city a reality IoT is essentially needed. 5th generation(5G) technology is needed for dealing with the huge amount of data and the requirement of high speed communication in the smart cities. 5G technology promises to provide the required data rate (>1 Gbps) and low latency (ms level) [1] with the use of low power small cells (e.g. microcells and picocells), it enhances the coverage and capacity of the network by spatial reuse of spectrum. There are limited options available in wireless techniques for the fulfilment of requirements of the 5G technique. Radio over free space optical (RoFSO) communication is one of the best available options for implementing 5G. It has many advantages like license free, high bandwidth, high data rate, easy deployment, low operating cost, immunity to electromagnetic interference and high security. Some of the applications of the RoFSO can be listed as fiber optic backup, last mile network access, high definition television (HDTV), cellular backhaul and temporary connectivity for many applications including voice, data, video and medical imaging [2, 3]. However, the performance of the RoFSO system depends on the atmospheric weather conditions.

As the RoFSO channel is the atmosphere, it has adverse effects, when the optical signal passing through the atmosphere. Thus, optical communication is prone to atmospheric attenuation, scintillation effects and scattering. The level of atmospheric attenuation depends on different weather conditions such as clear, haze, rain and fog etc. For example, the attenuation of the optical signal is minimum in clear, moderate in haze and maximum in fog weather conditions. Due to temperature variations in the atmosphere, the refractive index also gets varied and due to that the optical signal passing through it fluctuates, this effect is known as the scintillation effect and is also called turbulence induced fading. There are many mathematical models has been attempted to model this scintillation effect such as log-normal, negative exponential, K-distribution, Gamma–Gamma (GG) and M-distribution [4] etc. Malaga distribution or M-distribution is the generalized model because the other models are the special cases of this model and it almost accurately follows the experimental data from weak to strong turbulence.

Another deterioration factor for RoFSO is fading caused by misalignment, which happens due to unavoidable motion of the FSO transceiver, the reason for these motions can be strong wind, small

* Corresponding authors.
E-mail addresses: Abhishekranchi01@gmail.com (A. Kumar), prabuk@nitk.edu.in (P. Krishnan).

https://doi.org/10.1016/j.optcom.2020.125600
Received 13 January 2020; Accepted 20 February 2020
Available online 29 February 2020

earthquakes or thermal expansions. This misalignment fading can be categorized into two types i.e. Spatial jitter and fixed boresight displacement. In this work, the pointing errors are modeled using Beckmann and modified Rayleigh distributions. Thus, this model considers the non zero boresight displacement of the two vertical axes at each receiver and further different spatial jitters are also taken into consideration.

The effects of atmospheric turbulence and misalignment fading are reduced using many mitigation techniques like relay, diversity, multiple input multiple output, aperture averaging and robust modulation techniques. In this work, spatial diversity is used in which the maximum ratio combining (MRC) receiver is implemented. Here spatial diversity means multiple transmitters are used for the same signal transmission and each transmitter is transmitting toward a specific receiver [5].

There are many modulation schemes available like on off keying (OOK), pulse position modulation (PPM), subcarrier intensity modulation (SIM), pulse width modulation (PWM), phase shift keying (PSK), quadrature amplitude modulation (QAM) and polarization shift keying (PolSK), etc. [6,7]. In this work, we considered QAM orthogonal frequency division multiplexing (OFDM) as the robust modulation technique. OFDM is capable of transmitting signal parallelly by dividing it in the number of subcarriers which are orthogonal to each other. Thus, it offers less Intersymbol interference (ISI), high spectral efficiency and the prevention of selective frequency fading.

Different studies on QAM OFDM RoFSO link have been reported. In [8], the authors investigated the BER and outage probability performance of code division multiple access based RoFSO communication system for both forward and reverse direction over M-distribution channel with pointing errors. An OFDM RoFSO link is investigated with nonzero boresight pointing errors and spatial diversity over the GG atmospheric turbulence in [9]. The BER and outage probability results are analyzed for different spatial jitter variations. In [10], the authors studied the BER performance of the multi-hop RoFSO OFDM system using the PSK modulation scheme over the M-turbulence channel model with pointing errors for different weather conditions. A coherent optical OFDM based RoFSO transmission link integrating mode division multiplexing of Hermite-Gaussian modes using QAM and differential quadrature phase shift keying modulation scheme is demonstrated in [11]. The author improved the link range and information capacity of RoFSO links with the help of the proposed technique. In [12], the author studies the performance of PSK modulated OFDM FSO system over Gamma–Gamma distribution with misalignment fading for 5G applications. In this work, we analyzed the BER performance of QAM OFDM RoFSO link over M turbulence channel with pointing errors. We derived a novel BER expression for the proposed system. The BER results are analyzed and plotted for different weather conditions, various levels of turbulence regimes and pointing errors. Also, the BER performance is enhanced using spatial diversity with the MRC technique.

The rest of this work is organized as follows: In Section 2 the system details have been discussed, Section 3 describes the atmospheric channel model with pointing errors. In Section 4, the average BER of the K-QAM RoFSO link has been derived in the closed form mathematical expressions. In Section 5, numerical results are presented for different turbulence conditions, weather conditions with the combinations of spatial diversity and different misalignments. At the end in Section 6, the conclusion of this work has been summarized.

2. System model

In Fig. 1 architecture has been shown in which RoFSO has been used in the 5G network. In this figure, the central office connects different cells to the backhaul network which decreases energy consumption and cost. Here RoFSO is shown as last mile connectivity. RoFSO can be helpful for both the urban area and rural area. RoFSO is mainly proposed where the installation of optical fiber is much costly or it is going to take much time.

The spatial diversity is introduced in the RoFSO as a mitigation technique to reduce the adverse effect of the atmosphere. It improves the performance characteristics of the OFDM RoFSO link. Here the same signal is sent through M number of laser sources at the same moment. Every source is directed towards a specific receiver as you can see in Fig. 2. They are kept at some distance to be uncorrelated [5,13]. The free space channel is considered as stationary and memoryless with the parameters values having the same for all optical channels. We have considered intensity modulation with direct detection. Channel state information is available at both transmitting and receiving end.

The OFDM signal which is applied to laser source is firstly upconverted to the carrier frequency fc is given by [3]

$$S_{OFDM} = \sum_{n=0}^{N-1} S_n(t) = \sum_{n=0}^{N-1} X_n exp\left[i2\pi(\frac{n}{T_s} + f_c)t\right] \quad (1)$$

for $0 \le t < T_s$

Here T_s is the OFDM symbol period, N is the number of subcarriers, and X_n denotes the complex data symbol of the n_{th} subcarrier which is having modulation format of QAM. As the inverse fast Fourier transform (IFFT) output is bipolar so, to maintain the unipolarity of OFDM DC bias is added before it fed into the driving circuit of the laser source. The transmitted optical power from each laser source $P_t(t)$ can be given as [9].

$$P_t(t) \approx P_0\left[1 + \sum_{n=0}^{N-1} m_n S_n(t) + a_3\left(\sum_{n=0}^{N-1} m_n S_n(t)\right)^3\right] \quad (2)$$

Here P_0 stands for average transmitted power in the optical domain, a_3 stands for third order nonlinear coefficient and m_n represents the optical modulation index for each OFDM subcarrier. The optical OFDM signal travels through free space thus the transmitted power gets reduced as it travels through medium and also noise gets added to it. At the receiving end, the received power is given as [14]

$$P_{r,m}(t) = P_t(t)I + n_m(t) \quad (3)$$

Here I denotes the channel attenuation due to path loss, atmospheric turbulence and misalignment fading. Here $n_m(t)$ is the additive white Gaussian noise (AWGN) which gets added while traveling. By using Eqs. (2) and (3), following expression is obtained for the output current, $i_m(t, I)$, of each spatial diversity branch [3,14]

$$i_m(t, I) \approx I_{ph,m}\left[1 + \sum_{n=0}^{N-1} m_n s_n(t) + a_3\left(\sum_{n=0}^{N-1} m_n s_n(t)\right)^3\right] + n_{opt,m}(t) \quad (4)$$

Here $I_{ph,m} = \rho_m P_0 I_m$ represents the DC part of the photocurrent which is produced after receiving the signal, in each diversity branch. Another important degradation component is the intermodulation distortion (IMD) which originates from the nonlinear response of the laser source. The IMD noise of every subcarrier for OFDM in a particular diversity branch is given as [15]

$$\sigma^2_{n,IMD,m} = 2\zeta\left(2n(N-n+1) + N(N-5) + 2 - \frac{(-1)^n - (-1)^{2N+n}}{2}\right)^2 \quad (5)$$

The power of the signal after received by the photodetector for a particular subcarrier frequency is $C_{n,m}(I_m) = \frac{m_n^2 I_{ph,m}^2}{2}$. The instantaneous carrier to noise plus distortion ratio ($CNDR$) for a particular OFDM subcarrier which is calculated at the output of m_{th} receiver is given as [14]

$$CNDR_{n,m}(I_m) = \frac{(m_n \rho_m P_0 I_m)^2}{2(N_{0,m}/T_s + \sigma^2_{n,IMD,m})} \quad (6)$$

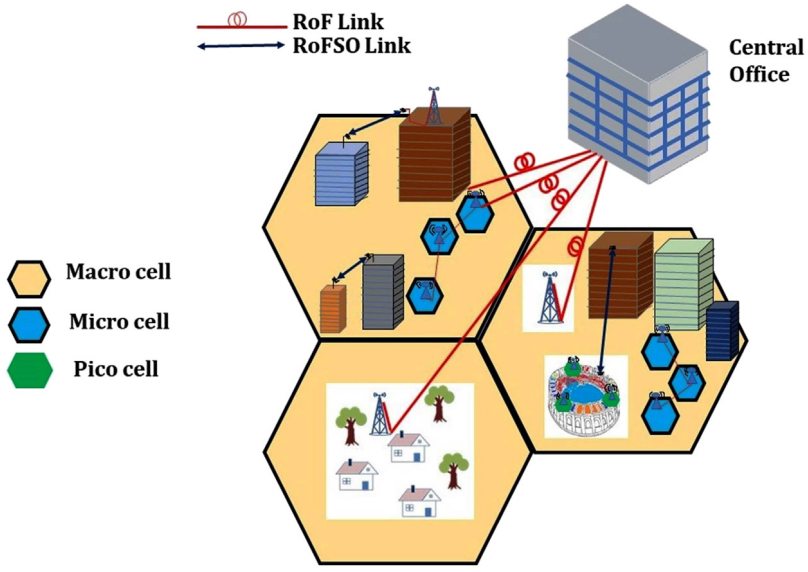

Fig. 1. FSO-based fronthaul network for 5G cells.

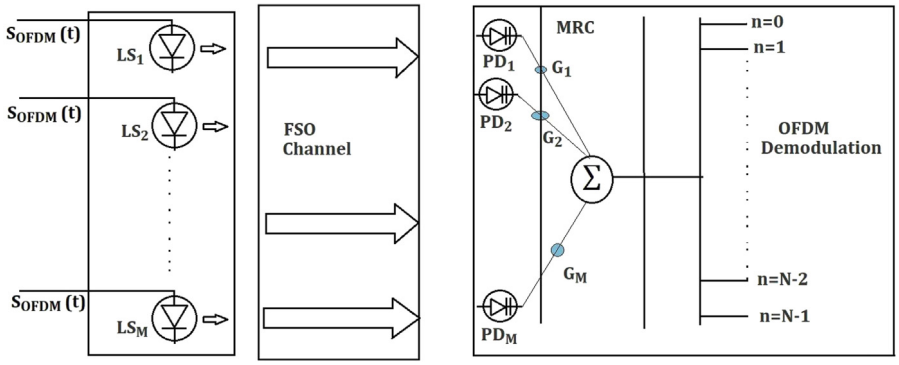

Fig. 2. Schematic representation of the spatially diverse OFDM RoFSO link.

Considering the IMD noise as Gaussian distributed [14] then Eq. (6) can be expressed as

$$CNDR_{n,m}(I_m) \approx \frac{m_n^2 \rho_m^2 P_0^2 I_m^2}{2[(N_{0,m}/T_s)_{AV} + (\sigma^2_{n,IMD,m})_{AV}]} \tag{7}$$

Here the AV stands for the average value. From Eq. (7) the expected value of $CNDR_{n,m}$ can be expressed as

$$CNDR_{n,m}(I_m) \approx \frac{m_n^2 \rho_m^2 P_0^2 (E[I_m])^2}{2[(N_{0,m}/T_s)_{AV} + (\sigma^2_{n,IMD,m})_{AV}]} \tag{8}$$

Here $E[I_m]$ is the expected value of I_m.

3. Channel model

In this work, the optical channel model I_m is taken as product of I_{am}, I_{pm} and I_{lm}, so we have [16]

$$I_m = I_{am} I_{lm} I_{pm} \tag{9}$$

Here, I_{am} is for atmospheric turbulence, I_{lm} is for atmospheric loss and I_{pm} is for pointing errors.

3.1. Atmospheric loss

To model the atmospheric loss Beer–Lambert's law [16] is used, thus we have

$$I_{lm} = exp(-\sigma L) \tag{10}$$

Table 1
Different attenuation coefficients at 1550 nm.

Weather condition	Attenuation σ (dB/KM)
Very clear air	0.0647
Haze	0.7360
Light fog	4.2850

Here L represents the link length and σ represents the attenuation coefficient. The value of σ changes according to atmospheric conditions. For 1550 nm wavelength optical signal different values of σ for different weather conditions are taken from [15] and these values have been given in Table 1. In this work, 3 km link length is taken.

3.2. Atmospheric turbulence induced fading

In the present work, free space optical (FSO) channel is modeled by Malaga distribution. In this M-distribution model, the optical beam is considered to have three components because of scattering, first is the line of sight (LOS) component having power Ω which is shown as route (A) in Fig. 3, second is the scattered component which is coupled to LOS and having power $2\rho b_0$ which is shown as route (B) in Fig. 3 and the third component is separate from former components having power $2(1-\rho)b_0$ which is shown as the route (C) in Fig. 3. Thus, the scattered component is having $2b_0$ total power. The coupling between the LOS and the scattered components is represented by ρ in this model. For

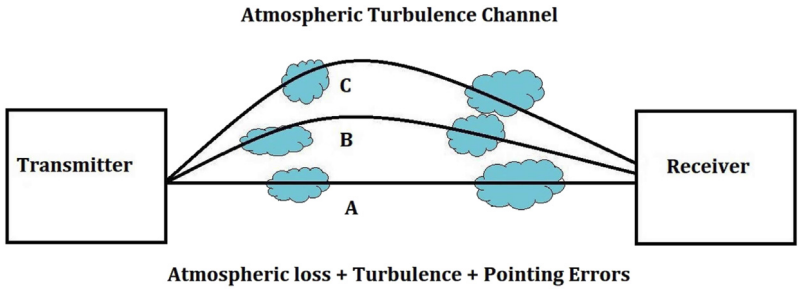

Fig. 3. Optical beam propagation in Malaga model [17].

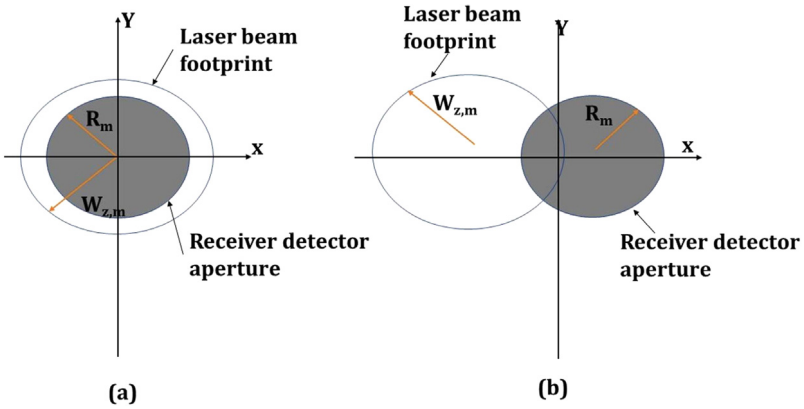

Fig. 4. RoFSO link (a) without pointing error (b) with pointing error.

the M-distribution turbulence the probability density function(PDF) is given by [16]

$$f_{I_{am}}(I_{am}) = A_m \sum_{k=1}^{b} a_{k_m} I_{am}^{\frac{\alpha_m+k}{2}-1} K_{\alpha_m-k}\left(2\sqrt{\frac{\alpha_m\beta_m I_{am}}{\gamma\beta_m+\Omega}}\right) \tag{11}$$

where

$$A_m = \frac{2\alpha_m^{\frac{\alpha_m}{2}}}{\gamma^{1+\frac{\alpha_m}{2}}\Gamma(\alpha_m)}\left(\frac{\gamma\beta_m}{\gamma\beta_m+\Omega'}\right)^{\beta_m+\frac{\alpha_m}{2}}$$

$$a_{k_m} = \binom{\beta_m-1}{k-1}\frac{(\gamma\beta_m+\Omega')^{1-\frac{k}{2}}}{k-1!}\left(\frac{\Omega'}{\gamma}\right)^{k-1}\left(\frac{\alpha_m}{\beta_m}\right)^{\frac{k}{2}}$$

α_m and β_m are the fading parameters. Here α_m represents a positive parameter of the scattering process which is related to large scale cells of this process. For generalized expression β_m can be derived as a real number, but it has a high degree of freedom in the proposed distribution thus not much of the interest. Here β_m is considered to be a natural number so that the PDF follows accurately with the practical observed data and also it leads to closed form representation [18]. Here $\gamma = 2(1-\rho)b_0$. Parameter $\Omega' = \Omega + 2\rho b_0 + 2\sqrt{2b_0\Omega\rho}cos(\phi_A - \phi_B)$ which is the average power received by the coherent contributions. Here ϕ_A is the phase of the LOS component and ϕ_B is phase of coupled-to-LOS scatter components. We have taken the difference between ϕ_A and ϕ_B is equal to 90°.

3.3. Pointing errors

The FSO communication system is primarily based on LOS. So, both the transmitter and receiver required to be highly aligned to each other, this alignment factor plays a primary role in the performance of the link. There are different reasons for the misalignment to happen e.g. by thermal expansions, wind loads and weak earthquakes [19–21] etc. These misalignments are called pointing errors as shown in Fig. 4. we have denoted these pointing errors as I_p and are generally be modeled as in Eq. (11), which considers the case of non zero boresight displacement. The PDF of distribution is given as [22]

$$f_{I_{pm}} = \frac{g^2}{A_0^{g^2}}(I_{pm})^{g^2} \qquad for \;\; 0 \le I_p \le A_0 \tag{12}$$

where $A_0 = [erf(v)]^2$ is the portion of the total received optical power. v is given by $v = \sqrt{\frac{\pi}{2}}\frac{a}{w_z}$, here a is radius of the receiver and w_z is the beam width of the transmitted optical signal at the distance L. Following expression is for the effective beam width at the receiving end.

$$w_{zeq} = \left[\frac{\sqrt{\pi}erf(v)w_z^2}{2ve^{-v^2}}\right]^{\frac{1}{2}} \tag{13}$$

Here $g = \frac{w_{zeq}}{2\sigma}$ is the ratio between the effective beam width and the jitter standard deviation σ.

3.4. Combined channel model

The overall channel model for I_m is given as [16]

$$f_{I_m}(I_m) = \int f_{I_m/I_{am}}(I_m/I_{am}) f_{I_{am}}(I_{am}) dI_{am} \tag{14}$$

Here $f_{I_m/I_{am}}(I_m/I_{am})$ is a conditional probability for a given turbulence state I_{am}. It is defined as

$$\begin{aligned} f_{I_m/I_{am}}(I_m/I_{am}) &= \frac{1}{I_{am}I_{lm}} f_{I_{pm}}\left(\frac{I_m}{I_{am}I_{lm}}\right) \\ &= \frac{g^2}{A_0^{g^2}I_{am}I_{lm}}\left(\frac{I_m}{I_{am}I_{lm}}\right)^{g^2-1} \end{aligned} \tag{15}$$

for $0 \le I_m \le A_0 I_{am} I_{lm}$

by substituting Eqs. (11) and (15) in (14) we have

$$f_{I_m}(I_m) = \frac{g^2 A}{(A_0 I_{lm})^{g^2}} (I_m)^{g^2-1} \times \sum_{k=1}^{b} a_{k_m} \int_{I_m/I_{lm}A_0}^{\infty} I_{am}^{\frac{\alpha_m+k}{2}-1-g^2} K_{\alpha_m-k}\left(2\sqrt{\frac{\alpha_m\beta_m I_{am}}{\gamma\beta_m+\Omega}}\right) dI_{am} \tag{16}$$

Final $f_{I_m}(I_m)$ can be obtained below [16]

$$f_{I_m}(I_m) = \frac{g^2 A_m I_m^{-1}}{2} \sum_{k=1}^{\beta} \left[\left(a_{k_m} B_m^{\frac{\alpha_m+k}{2}}\right) G_{1,3}^{3,0}\left(\frac{I_m}{B_m A_0 I_{lm}}\middle| \begin{matrix} 1+g^2 \\ g^2, \alpha_m, k \end{matrix}\right)\right] \tag{17}$$

where $B_m = \frac{\Omega+\gamma_m\beta}{\alpha_m\beta_m}$ and $G_{p,q}^{m,n}[\ .\ ]$ is meijer G function.

4. The average BER of the RoFSO system

Wireless communication system performance can be determined by knowing the BER. CNDR is a major parameter that has a role in determining the BER. Thus, in this section, we find the average BER with the help of CNDR per subcarrier for the RoFSO communication link which is spatially diverse. We have calculated average BER after the received signal combined through MRC combiner. Here we have also taken account of the atmospheric turbulence with the non zero boresight pointing errors and atmospheric losses. we can estimate the average BER $P_{n,MRC,AV}$ of the K-QAM OFDM RoFSO link for each particular subcarrier through expression [23]

$$p_{n.MRC,AV} = \int_{I_m} f_{I_m}(I_m) P_{n,QAM,MRC}(I_m) dI_m \tag{18}$$

Following equation gives the conditional BER for the K-QAM modulation. Here spatial diversity and MRC combiner has also been taken into account and the conditional BER is calculated for each subcarrier [15]:

$$p_{n.MRC,QAM}(I_m) = \frac{4(1-K^{\frac{-1}{2}})}{log_2(K)} Q\left(\sqrt{\frac{3}{K-1}\sum_{m+1}^{M} CNDR_{N.M}(I_m)}\right) \tag{19}$$

We have used the following approximation for the Q function [24]

$$Q(x) \approx \frac{1}{24}\left[5exp(-2x^2) + 4exp\left(-\frac{11x^2}{20}\right) + exp\left(-\frac{x^2}{2}\right)\right] \tag{20}$$

Now we substitute the Eq. (20) into (19) and used its outcome in Eq. (18), as the I_m is not depend on each other the multiple integral of Eq. (18) become summation of products of single dimensional integral [23]

$$P_{n,AV} \approx \frac{1-K^{-1/2}}{6log_2 K}\left[5\prod_{m=1}^{M}\int_0^{\infty} f_{I_m}(I_m)exp(-2y)dI_m + 4\prod_{m=1}^{M}\int_0^{\infty} f_{I_m}(I_m)exp(-\frac{11y}{20})dI_m + \prod_{m=1}^{M}\int_0^{\infty} f_{I_m}(I_m)exp(-\frac{y}{2})dI_m\right] \tag{21}$$

where $y = \frac{3CNDR_{n,m}(I_m)}{(K-1)}$

Now, we substitute the combined channel fading model into the average BER of each subcarrier i.e. substituting Eq. (17) into (21). While doing this we transform the exponential terms present in Eq. (21) into the Meijer-G function and solved the integrals with the help of [25]. Thus, we get the closed form mathematical Eq. (22). This expression is for the calculation of average BER of individual subcarrier from within N subcarriers. For this expression K-QAM OFDM RoFSO link, M-receivers diversity is considered.

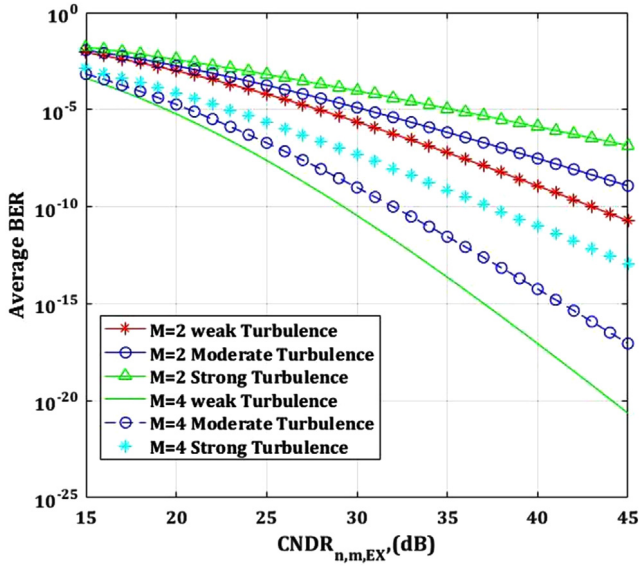

Fig. 5. Average BER in terms of the electrical $CNDR_{n,m,EX}$ per diversity order for different turbulence conditions.

$$P_{n,AV} \approx \frac{1-K^{-1/2}}{6log_2 K}\left(5\phi(2,M) + 4\phi(\frac{11}{20},M) + 4\phi(0.5,M)\right) \tag{22}$$

where $\phi(x,M) = \prod_{m=1}^{M} \Lambda(m)\psi(x,m)$

$$\Lambda(m) = \frac{g_m^2 A_m}{2} \quad and$$

$$\psi(x,m) = \sum_{k=1}^{\beta_m}\left[a_{k_m} B_m^{\frac{\alpha_m+k}{2}} \frac{2^{(\alpha_m+k-2)}}{2\pi} G_{1,6}^{6,3}\left(z\middle|\begin{matrix}\eta \\ \chi\end{matrix}\right)\right]$$

where $z = \frac{48xCNDR_{n,m,EX}(1+g^{-2})^2 B_m^2 I_{lm}^2}{K-1}$ $\eta = \frac{1-g^2}{2}, \frac{2-g^2}{2}, \frac{1-\alpha_m}{2}, \frac{2-\alpha_m}{2}, \frac{1-k}{2}, \frac{2-k}{2}$ and $\chi = 0, \frac{-g^2}{2}, \frac{1-g^2}{2}$

The $CNDR_{n,m,EX}$ is taken from (8) and the expected value of I_m can be given as [26]

$$E[I_m] = \int_0^{\infty} I_m f_{I_m}(I_m) dI_m = A_0(1+g^{-2})^{-1} \tag{23}$$

After taking high number of subcarriers [14] the average BER of the K-QAM OFDM RoFSO link with spatial diversity and M-distribution model is given as

$$P_{AV} \approx \frac{1-K^{-1/2}}{6Nlog_2 K}\sum_{n=0}^{N-1}\left(5\phi(2,M) + 4\phi(\frac{11}{20},M) + 4\phi(0.5,M)\right) \tag{24}$$

5. Numerical results

From the derived mathematical expressions of average BER Eqs. (22) and (24), the result is presented. The link length we have taken as L = 3 km. we assumed that the aperture of all the receivers is having the same radius i.e. 5 cm. And the working wavelength of the optical signal is $\lambda = 1.55$ μm. The above mentioned points are the same for all links in the spatially diverse system. So, we have α_m and β_m of each individual link is taken as equal. For pointing errors also, the same parameter values are taken. The symbol C_n^2 represents the refractive index structure parameter and its value depends on the atmospheric turbulence

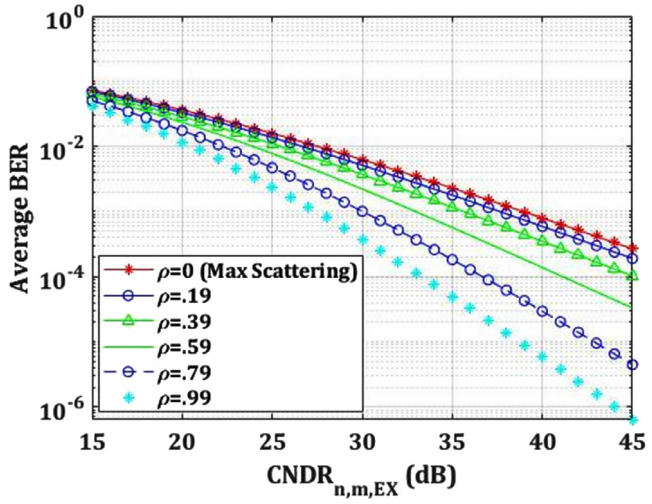

Fig. 6. Average BER in terms of the electrical $CNDR_{n,m,EX}$ per diversity order for various ρ values at strong turbulence.

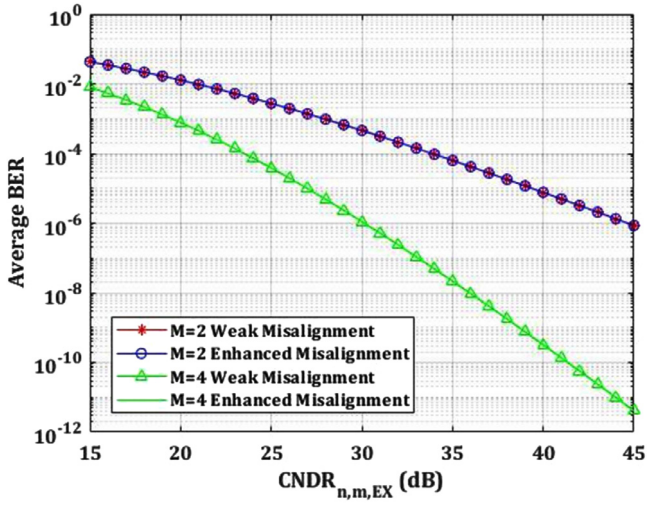

Fig. 7. Average BER in terms of the electrical $CNDR_{n,m,EX}$ per diversity order for various misalignment at strong turbulence.

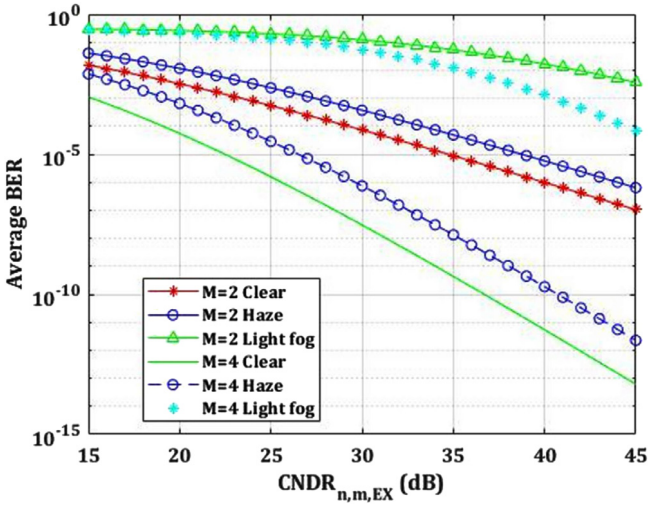

Fig. 8. Average BER in terms of the electrical $CNDR_{n,m,EX}$ per diversity order for various weather conditions at strong turbulence.

strength. C_n^2 is taken as 2×10^{-14} $m^{-2/3}$ for weak , 4×10^{-14} $m^{-2/3}$ for moderate and 8×10^{-14} $m^{-2/3}$ for strong turbulence Conditions. α_m and β_m are calculated from the expression given in [9]. For investigating nonzero boresight pointing error effect we have taken two cases, first is weak misalignment and second is enhanced misalignment. In the weak misalignment, we consider normalized spatial jitter $(\sigma_{x.m}/R_m, \sigma_{y.m}/R_m)$ = (0.2, 0.1) and zero boresight displacement $(\mu_{x.m}/R_m, \mu_{y.m}/R_m)$ = (0, 0). In the enhanced misalignment, we consider normalized spatial jitter $(\sigma_{x.m}/R_m, \sigma_{y.m}/R_m)$ = (0.5, 0.2) and non zero boresight displacement $(\mu_{x.m}/R_m, \mu_{y.m}/R_m)$ = (0.2, 0.2). Here R_m is the aperture radius of each receiver. The waist of the transmitted beam is taken as $W_{0,m}$ = 4 cm.

For plotting Fig. 5, we have considered 16-QAM RoFSO link with spatial diversity, weak misalignment and clear weather conditions. It is evident from the plot that an average BER of 10^{-6} or lower values are achieved at 30 dB CNDR for all three turbulence conditions with M = 4 and an average BER of 10^{-4} or lower values are achieved at 30 dB CNDR for all three turbulence conditions with M = 2. So, it is concluded that as we increase the diversity branch the performance enhances rapidly.

For Fig. 6 we have considered 16-QAM RoFSO link with spatial diversity of M = 2, weak misalignments, and Haze weather conditions. Here we have taken strong turbulence. The effect of scattering increases as the value of CNDR increases. For example for ρ = .99 (min. Scattering) 10^{-3} BER is achieved at 27 dB CNDR but for same BER ρ = 0 (Max. Scattering) needed 39 dB CNDR which is 12 dB more requirement to achieve the same BER.

Different considerations for plotting Fig. 7 are 16-QAM RoFSO link with spatial diversity and haze weather conditions. Here strong turbulence condition has been considered. It is clearly visible from Fig. 7 that the weak and enhanced misalignment effect is minimal on the performance of the link in comparison to the effect of increasing the diversity branch in the link.

For Fig. 8 we have considered 16-QAM RoFSO link with spatial diversity and weak misalignment. Here we have taken strong turbulence. It is evident that the effect of weather conditions can overcome easily by increasing the diversity branch in the link as BER of 10^{-6} can be achieved at 39 dB CNDR for M = 2 clear weather but for the same BER only 30 dB CNDR is required for M = 4 Haze weather conditions. And for fog weather conditions the effect of increment of diversity branch is much less effective as till 30 dB CNDR the BER value is very near for both M = 2 and M = 4 fog conditions.

For Fig. 9 we have considered 16-QAM RoFSO link with spatial diversity M = 4 and weak misalignment. It is evident that the weather condition fog is having more effect than strong turbulence as from graph we can see that the BER value is very close for both in the whole plot of light fog with weak turbulence and light fog with strong turbulence. So, it can be concluded that in fog weather conditions the link performance is most affected.

For Fig. 10 we have considered RoFSO link with spatial diversity, weak misalignment, haze weather condition and strong turbulence. It is evident from Fig. 10 that as we increase the order of QAM i.e. as the data which is transmitting through the link get increased the BER also get increased and thus the performance of the link reduced, for example for 10^{-4} BER M = 2, 16-QAM required 33 dB CNDR, 64-QAM required 38 dB CNDR and 256-QAM required 45 dB CNDR.

6. Conclusion

In this work, we investigated the BER performance of K-QAM OFDM RoFSO link with spatial diversity. The channel model is considered as the combined one with the effects of atmospheric attenuation, turbulence and misalignment fading. The atmospheric turbulence and the pointing errors are modeled through M-distribution, Beckmann and modified Rayleigh distribution respectively. The novel closed form expression of the average BER is derived for the proposed system which is based on the M-distribution model which follows accurately

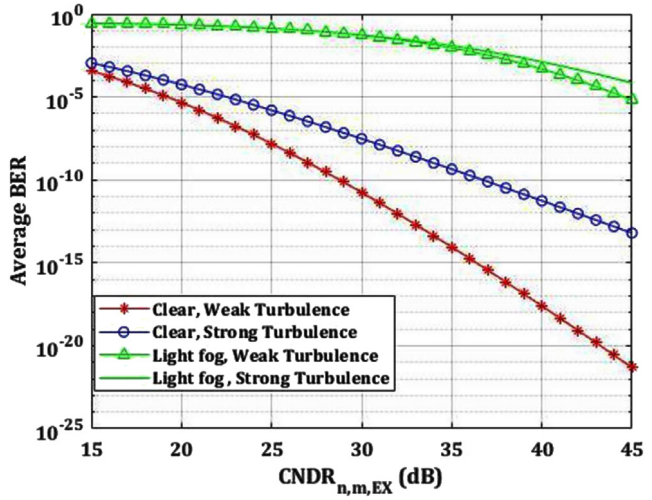

Fig. 9. Average BER in terms of the electrical CNDRn,m,EX per diversity order for various turbulence condition, and weather condition combinations.

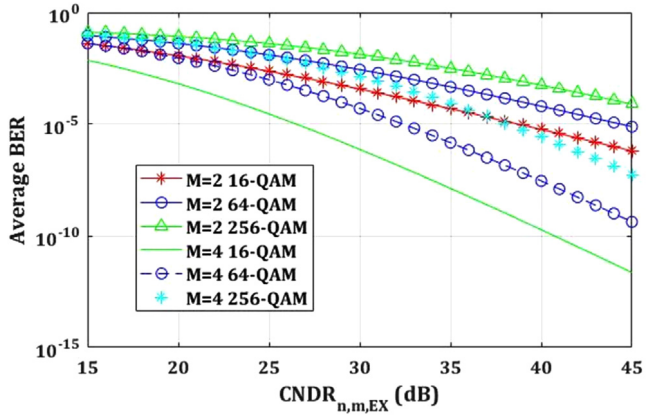

Fig. 10. Average BER in terms of the electrical$CNDR_{n,m,EX}$ per diversity order for various QAM at strong turbulences.

experimental observations. The results are analyzed and plotted for different weather, turbulence, and pointing error conditions. It can be concluded that the increment in the diversity branch enhances the performance of the link in great amount in all turbulence conditions. The proposed OFDM based RoFSO system is highly useful in smart cities and 5G applications. The complete analysis presented in the paper can be useful for the design engineers in designing a system, for smart city applications.

Funding

This work was supported by the Science and Engineering Research Board, India, Department of Science and Technology, Government of India, under Grant EEQ/2018/001107.

References

[1] O.N. Yilmaz, Y.-P.E. Wang, N.A. Johansson, N. Brahmi, S.A. Ashraf, J. Sachs, Analysis of ultra-reliable and low-latency 5g communication for a factory automation use case, in: 2015 IEEE international conference on communication workshop (ICCW), 2015, pp. 1190–1195, http://dx.doi.org/10.1109/ICCW.2015.7247339.

[2] G. Aarthi, K. Prabu, G. Reddy, Aperture averaging effects on the average spectral efficiency of fso links over turbulence channel with pointing errors, Opt. Commun. 385 (2017) 136–142, http://dx.doi.org/10.1016/j.optcom.2016.10.041.

[3] K. Kazaura, K. Wakamori, Matsumoto, Rofso: a universal platform for convergence of fiber and free-space optical communication networks, IEEE Commun. Mag. 48 (2) (2010) 130–137, http://dx.doi.org/10.1109/MCOM.2010.5402676.

[4] M.A. Kashani, M. Uysal, M. Kavehrad, A novel statistical channel model for turbulence-induced fading in free-space optical systems, J. Lightwave Technol. 33 (11) (2015) 2303–2312, http://dx.doi.org/10.1109/JLT.2015.2410695.

[5] R. Boluda-Ruiz, A. García-Zambrana, B. Castillo-Vázquez, C. Castillo-Vázquez, On the effect of correlated sways on generalized misalignment fading for terrestrial fso links, IEEE Photonics J. 9 (3) (2017) 1–14, http://dx.doi.org/10.1109/JPHOT.2017.2694707.

[6] H. Nistazakis, A. Stassinakis, S.S. Muhammad, G. Tombras, Ber estimation for multi-hop rofso qam or psk ofdm communication systems over gamma gamma or exponentially modeled turbulence channels, Opt. Laser Technol., 64, 106.

[7] H.E. Nistazakis, A.N. Stassinakis, H. Sandalidis, G. Tombras, Qam and psk ofdm rofso over M-turbulence induced fading channels, IEEE Photonics J. 7 (1) (2014) 1–11, http://dx.doi.org/10.1109/JPHOT.2014.2381670.

[8] M.P. Ninos, H.E. Nistazakis, H.G. Sandalidis, G.S. Tombras, Cdma rofso links with nonzero boresight pointing errors over m turbulence channels, IEEE Photonics J. 10 (5) (2018) 1–12, http://dx.doi.org/10.1109/JPHOT.2018.2856369.

[9] M.P. Ninos, H.E. Nistazakis, E. Leitgeb, G.S. Tombras, Spatial diversity for qam ofdm rofso links with nonzero boresight pointing errors over atmospheric turbulence channels, J. Mod. Opt. 66 (3) (2019) 241–251, http://dx.doi.org/10.1080/09500340.2018.1516828.

[10] K. Balaji, K. Prabu, Ber analysis of relay assisted psk with ofdm rofso system over malaga distribution including pointing errors under various weather conditions, Opt. Commun. 426 (2018) 187–193, http://dx.doi.org/10.1016/j.optcom.2018.05.027.

[11] M. Singh, J. Malhotra, Performance comparison of m-qam and dqpsk modulation schemes in a 2× 20 gbit/s–40 ghz hybrid mdm–ofdm-based radio over fso transmission system, Photonic Netw. Commun. 38 (3) (2019) 378–389.

[12] P.S. Pati, P. Krishnan, Modelling of ofdm based rofso system for 5g applications over varying weather conditions: A case study, Optik 184 (2019) 313–323, http://dx.doi.org/10.1016/j.ijleo.2019.03.031.

[13] J.-Y. Wang, J.-B. Wang, M. Chen, Y. Tang, Y. Zhang, Outage analysis for relay-aided free-space optical communications over turbulence channels with nonzero boresight pointing errors, IEEE Photonics J. 6 (4) (2014) 1–15, http://dx.doi.org/10.1109/JPHOT.2014.2332554.

[14] A. Bekkali, C.B. Naila, K. Kazaura, K. Wakamori, M. Matsumoto, Transmission analysis of ofdm-based wireless services over turbulent radio-on-fso links modeled by gamma–gamma distribution, IEEE Photonics J. 2 (3) (2010) 510–520, http://dx.doi.org/10.1109/JPHOT.2010.2050306.

[15] H. Al-Raweshidy, S. Komaki, Radio over fiber technologies for mobile communications networks, Artech House, 2002.

[16] P. Wang, R. Wang, L. Guo, T. Cao, Y. Yang, On the performances of relay-aided fso system over m distribution with pointing errors in presence of various weather conditions, Opt. Commun. 367 (2016) 59–67, http://dx.doi.org/10.1016/j.optcom.2016.01.004.

[17] K. Balaji, K. Prabu, Performance evaluation of fso system using wavelength and time diversity over malaga turbulence channel with pointing errors, Opt. Commun. 410 (2018) 643–651, http://dx.doi.org/10.1016/j.optcom.2017.11.006.

[18] A. Jurado-Navas, J.M.G. Balsells, J.F. Paris, M. Castillo-Vázquez, A. Puerta-Notario, General analytical expressions for the bit error rate of atmospheric optical communication systems, Opt. Lett. 36 (20) (2011) 4095–4097, http://dx.doi.org/10.1364/OL.36.004095.

[19] A.A. Farid, S. Hranilovic, Outage capacity optimization for free-space optical links with pointing errors, J. Lightwave Technol., 25(7).

[20] W. Gappmair, S. Hranilovic, E. Leitgeb, Performance of ppm on terrestrial fso links with turbulence and pointing errors, IEEE Commun. Lett. 14 (5) (2010) 468–470, http://dx.doi.org/10.1109/LCOMM.2010.05.100202.

[21] H.G. Sandalidis, T.A. Tsiftsis, G.K. Karagiannidis, Optical wireless communications with heterodyne detection over turbulence channels with pointing errors, J. Lightwave Technol. 27 (20) (2009) 4440–4445.

[22] P. Krishnan, U. Jana, B.K. Ashokkumar, Asymptotic bit-error rate analysis of quadrature amplitude modulation and phase-shift keying with ofdm rofso over m turbulence in the presence of pointing errors, IET Commun. 12 (16) (2018) 2046–2051, http://dx.doi.org/10.1049/iet-com.2017.0560.

[23] T.A. Tsiftsis, H.G. Sandalidis, G.K. Karagiannidis, M. Uysal, Optical wireless links with spatial diversity over strong atmospheric turbulence channels, IEEE Trans. Wireless Commun. 8 (2) (2009) 951–957, http://dx.doi.org/10.1109/TWC.2009.071318.

[24] Q. Zhang, J. Cheng, G.K. Karagiannidis, Block error rate of optical wireless communication systems over atmospheric turbulence channels, IET Commun. 8 (5) (2014) 616–625, http://dx.doi.org/10.1049/iet-com.2013.0164.

[25] V. Adamchik, O. Marichev, The algorithm for calculating integrals of hypergeometric type functions and its realization in reduce system, in: Proceedings of the International Symposium on Symbolic and Algebraic Computation, 1990, pp. 212–224.

[26] G. Varotsos, H. Nistazakis, M. Petkovic, G. Djordjevic, G. Tombras, Simo optical wireless links with nonzero boresight pointing errors over m modeled turbulence channels, Opt. Commun. 403 (2017) 391–400, http://dx.doi.org/10.1016/j.optcom.2017.07.055.